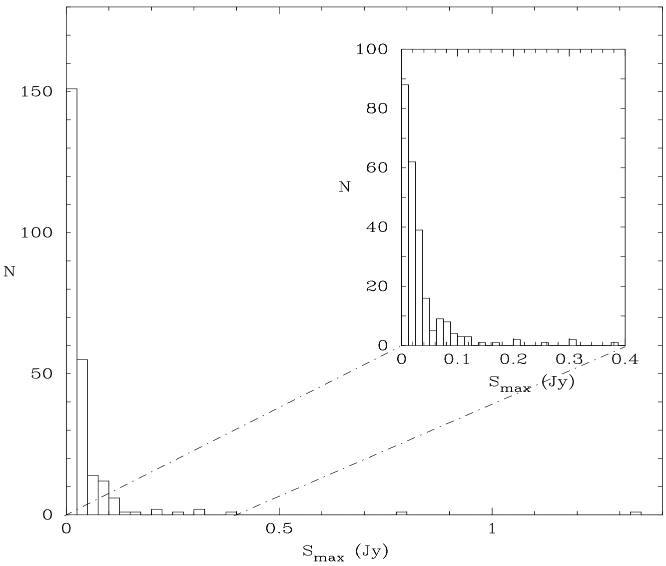

Figure 1: The flux density distribution of confusing sources in the IDV sample for 1.4 GHz. S_{max} is the maximum flux density in a confusing source. N corresponds to the number of confusing sources detected in 101 images of the IDV sample target sources (no beam shape correction applied).

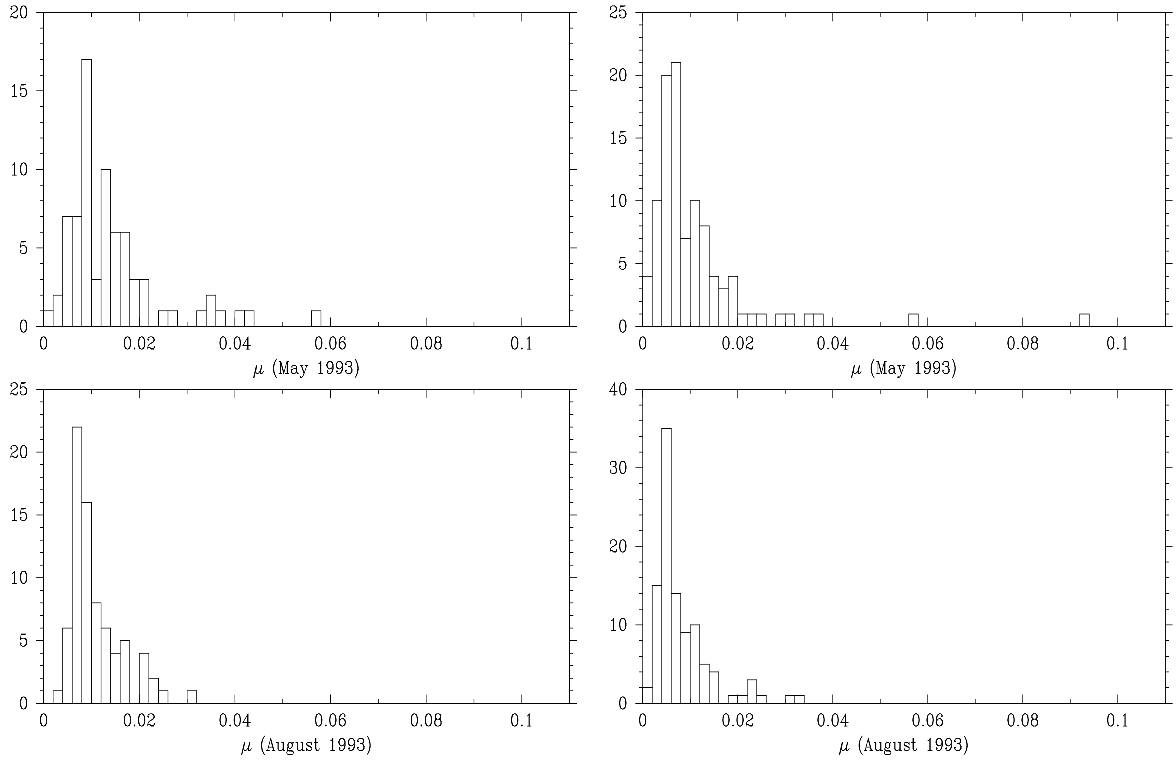

(a) 2.4 GHz (b) 4.8 GHz

Figure 2: The number distribution of modulation indices, μ of the total flux density calculated over the duration of each observing run: May 1994 and August 1994. The distributions of μ are shown for (a) 2.4 GHz and (b) 4.8 GHz. The distribution for November are significantly broader than for May and August.

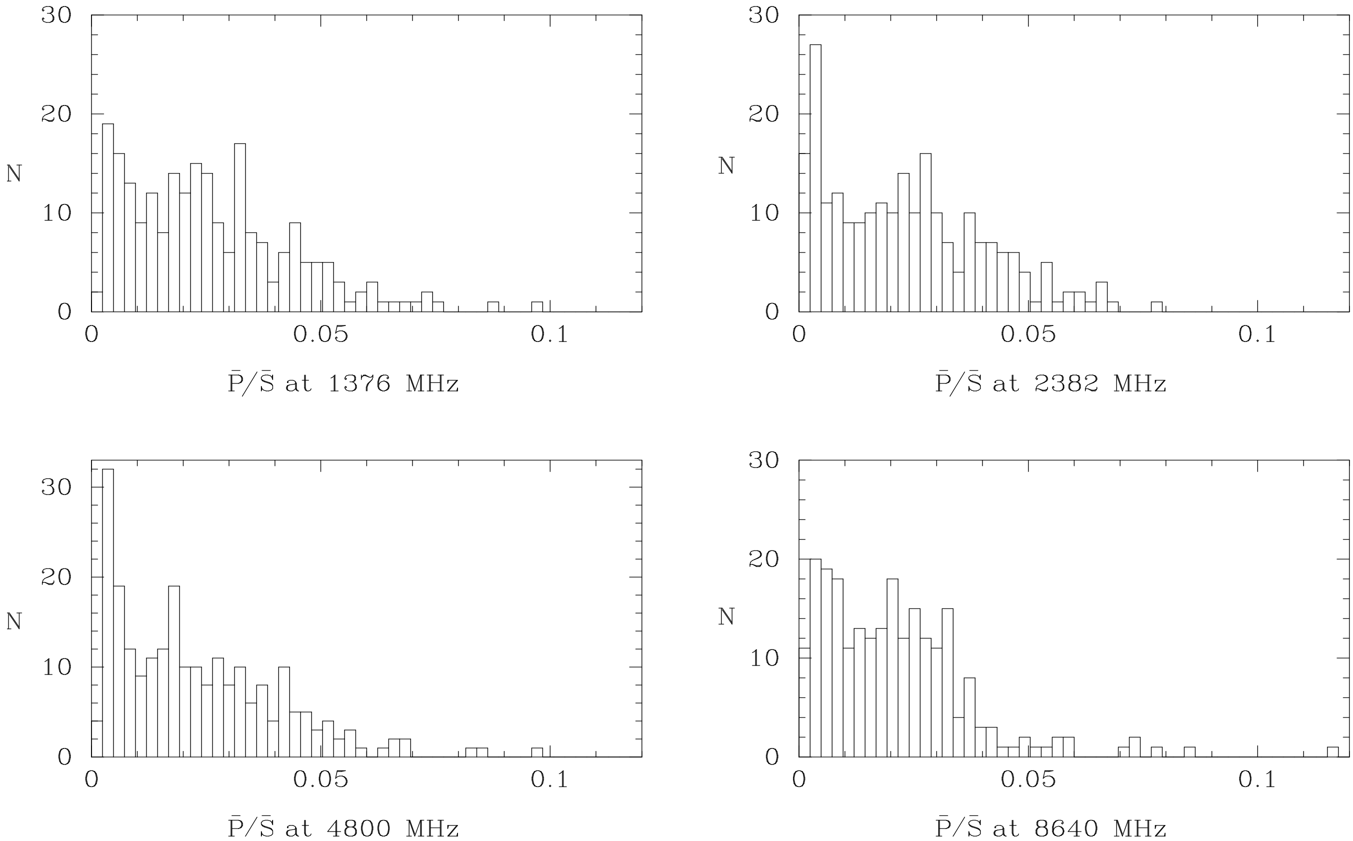

Figure 3: Distribution of the fractional linear polarization averaged over a duration of each observing session (May and August 1994) for all sources in the sample.

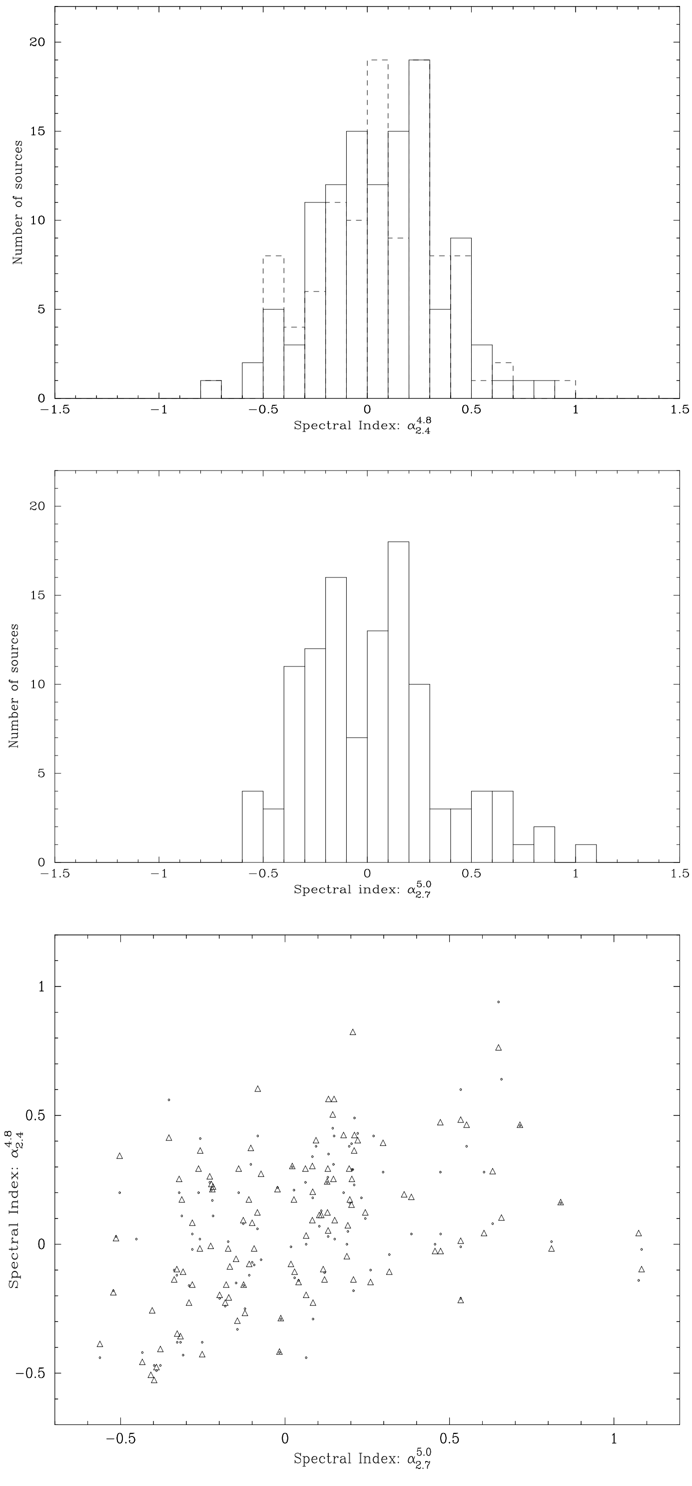

Figure 4: Upper panel: the number distribution of instantaneous spectral indices $\alpha_{2.4}^{4.8}$ of all sources for May 1994 (full line) and August 1994 (dashed line). Middle panel: the number distribution of the spectral indices $\alpha_{2.7}^{5.0}$ calculated from the flux densities provided in the Parkes catalogue. Lower panel: The scatter plot of Parkes spectral indices $\alpha_{2.7}^{5.0}$ versus instantaneous spectral indices $\alpha_{2.4}^{4.8}$ of all sources for May 1994 (dots) and August 1994 (triangles).

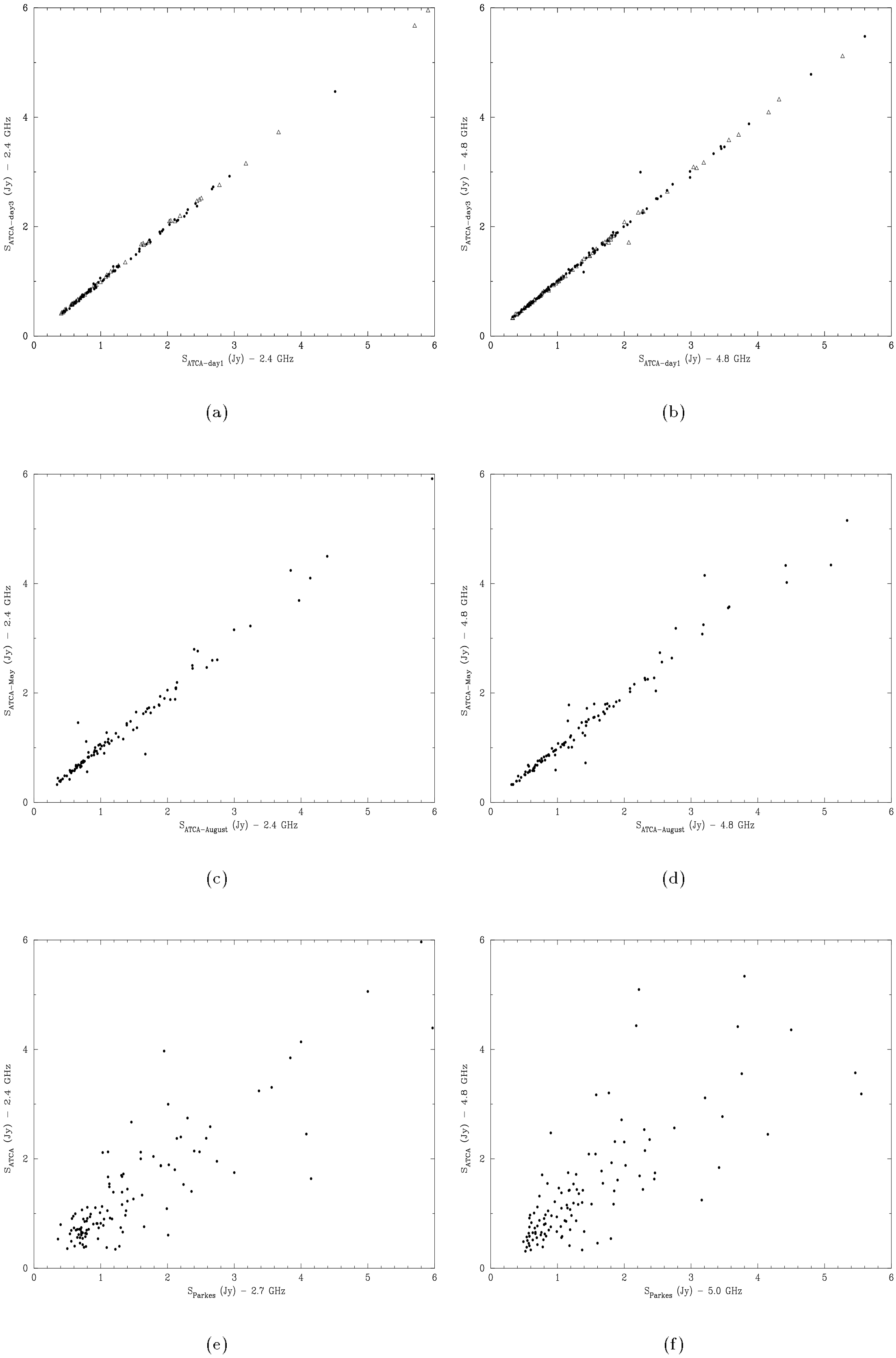

Figure 5: A comparison of flux densities measured at different times between days and decades. (a) and (b) show the scatter between the mean flux densities measured one day apart with the ATCA at 2.4 and 4.8 GHz respectively, triangles correspond to August 1994 data, dots are May 1994 data (c) and (d) are the scatter plots of average flux densities measured 3 months apart with the ATCA, (e) and (f) show flux densities measured with ATCA in May 1994 versus flux densities listed in the Parkes catalogue.

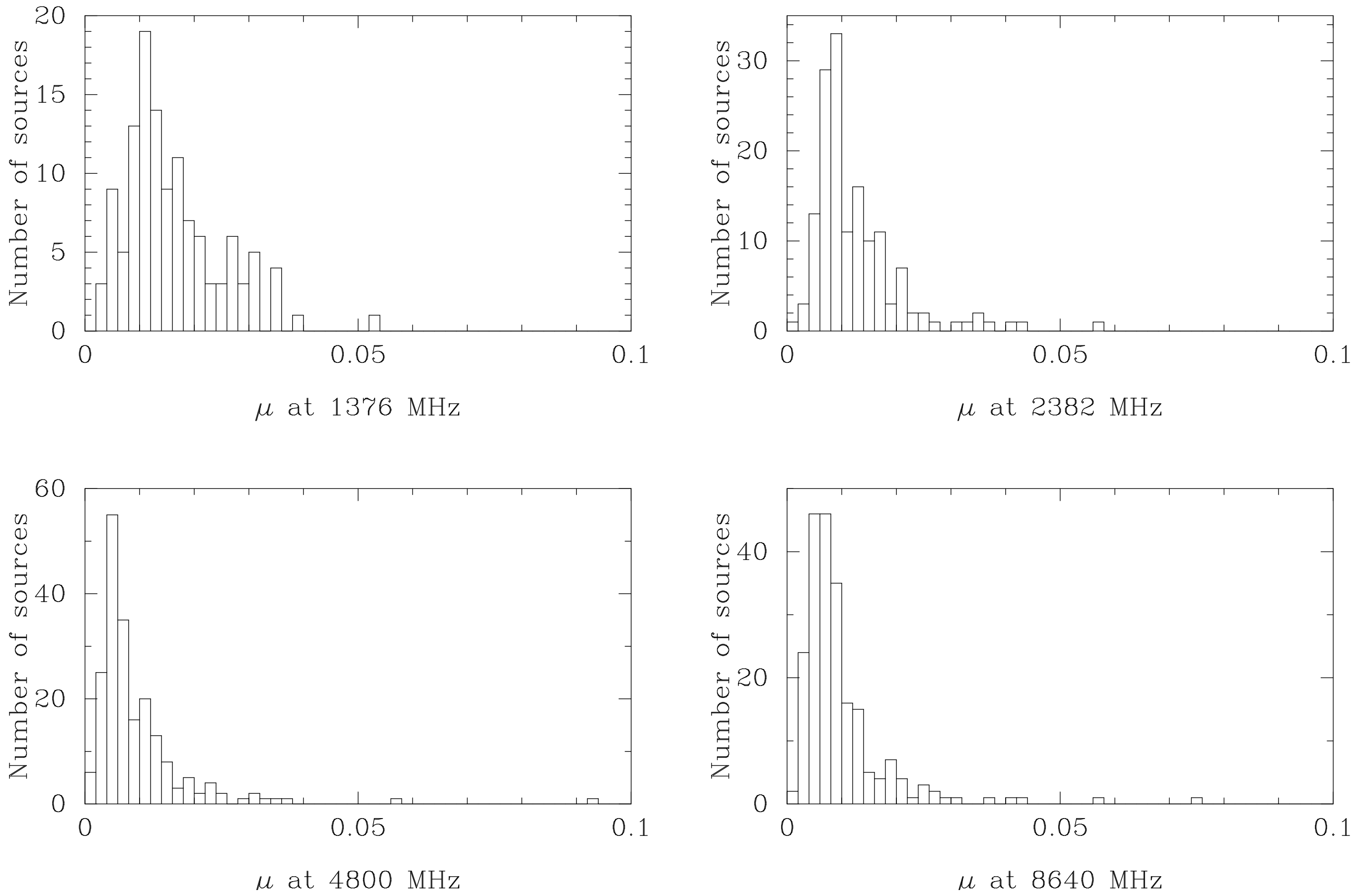

Figure 6: The distribution of modulation indices calculated over 72 hours. The distributions are combined over two observing sessions, May and August 1994 for all frequencies.

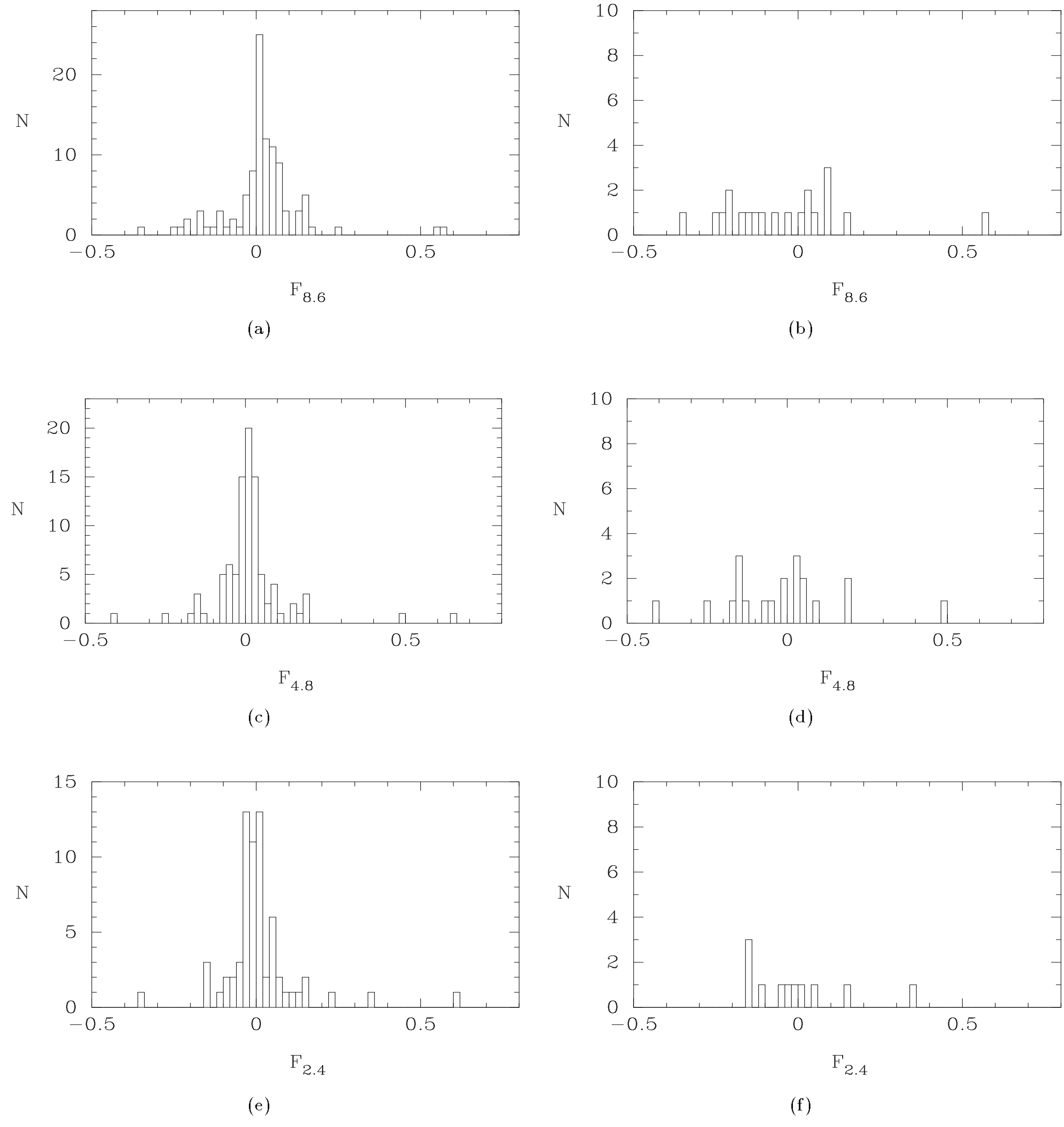

Figure 7: Distribution of the fractional difference in average flux density between two observing sessions in May and August 1994. Left panels: the data for the point sources in the Survey sample. Right panels: only IDV sources from table ?? are included.

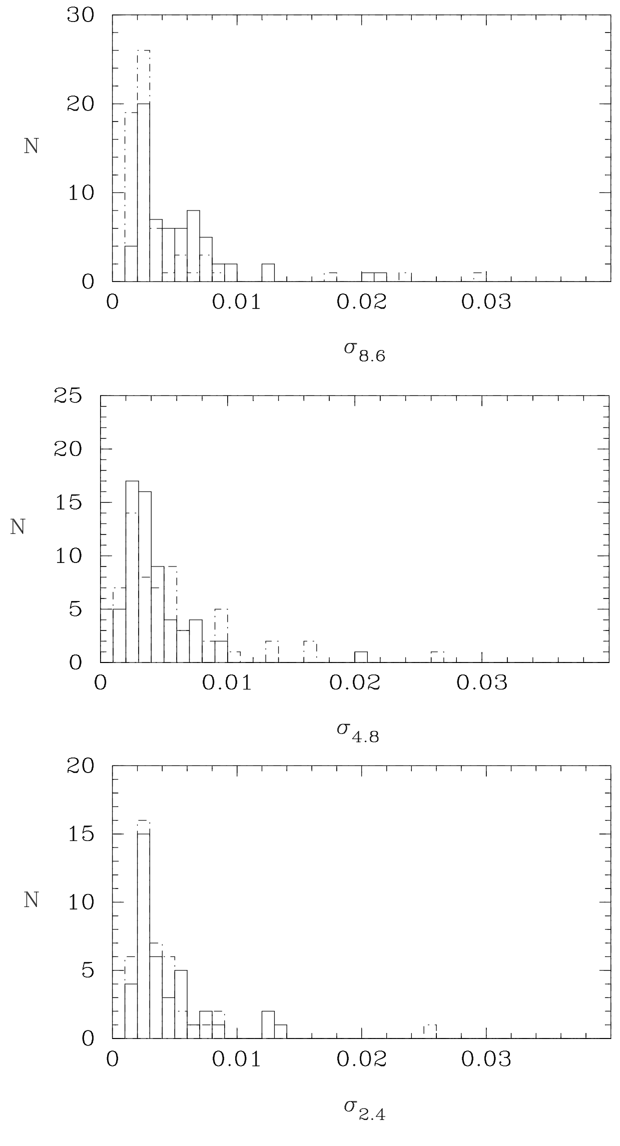

Figure 8: The number distribution of the rms in polarized flux densities at 8.6, 4.8 and 2.3 GHz from top to bottom.

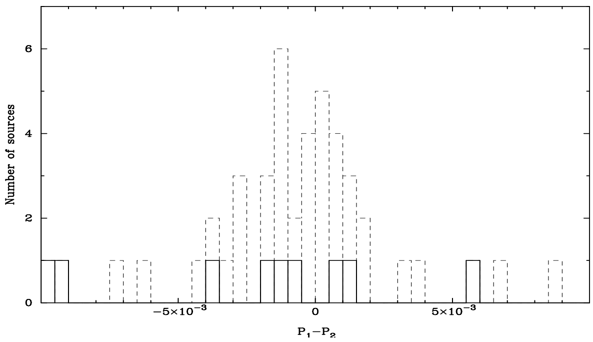

(a)

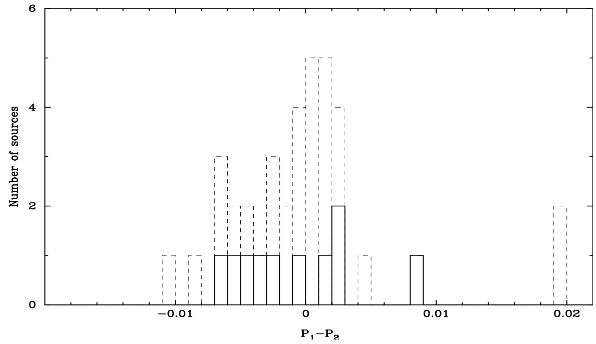

(b)

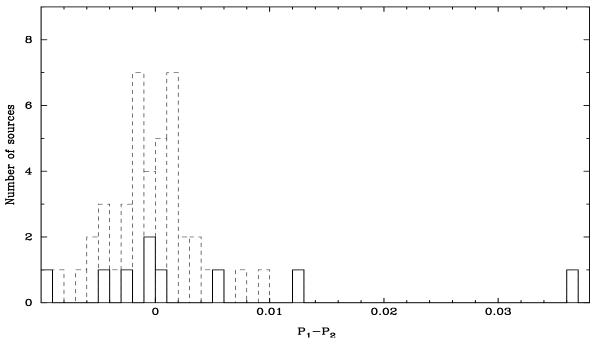

(c)

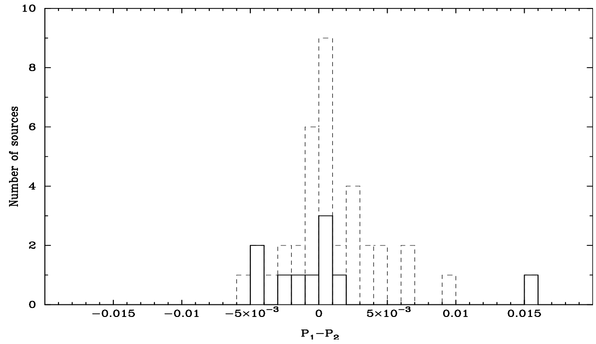

(d)

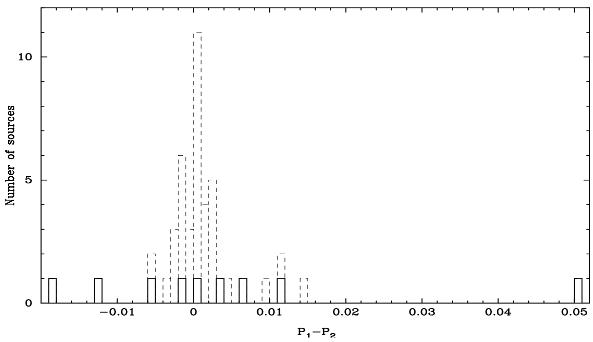

(e)

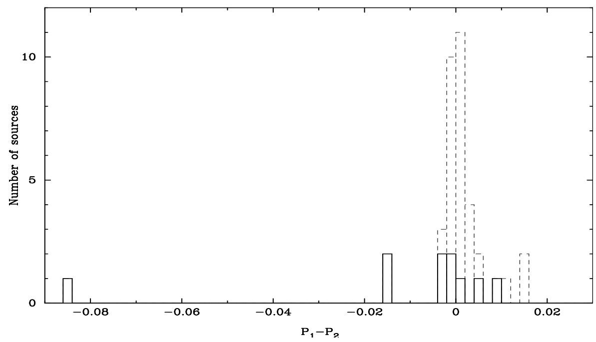

(f)

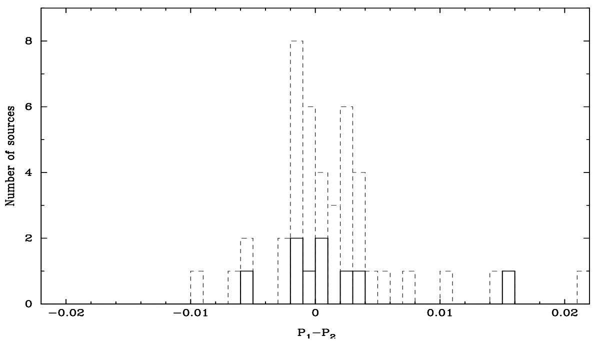

(g)

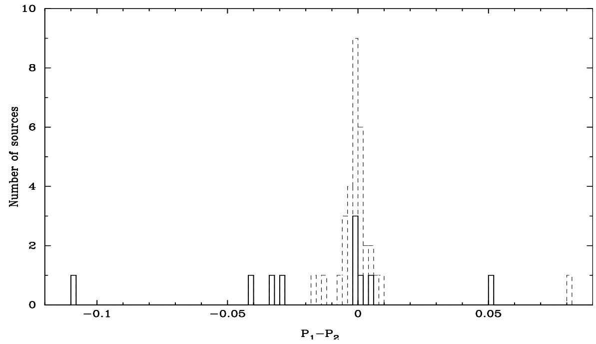

(h)

Figure 9: Distribution of day-to-day differences in polarized flux densities. Figures (a), (c), (e) and (g) show May 1994 data for 8.6, 4.8, 2.4 and 1.4 GHz respectively. Figures (b), (d), (f) and (h) show August 1994 data for frequencies in the same order.

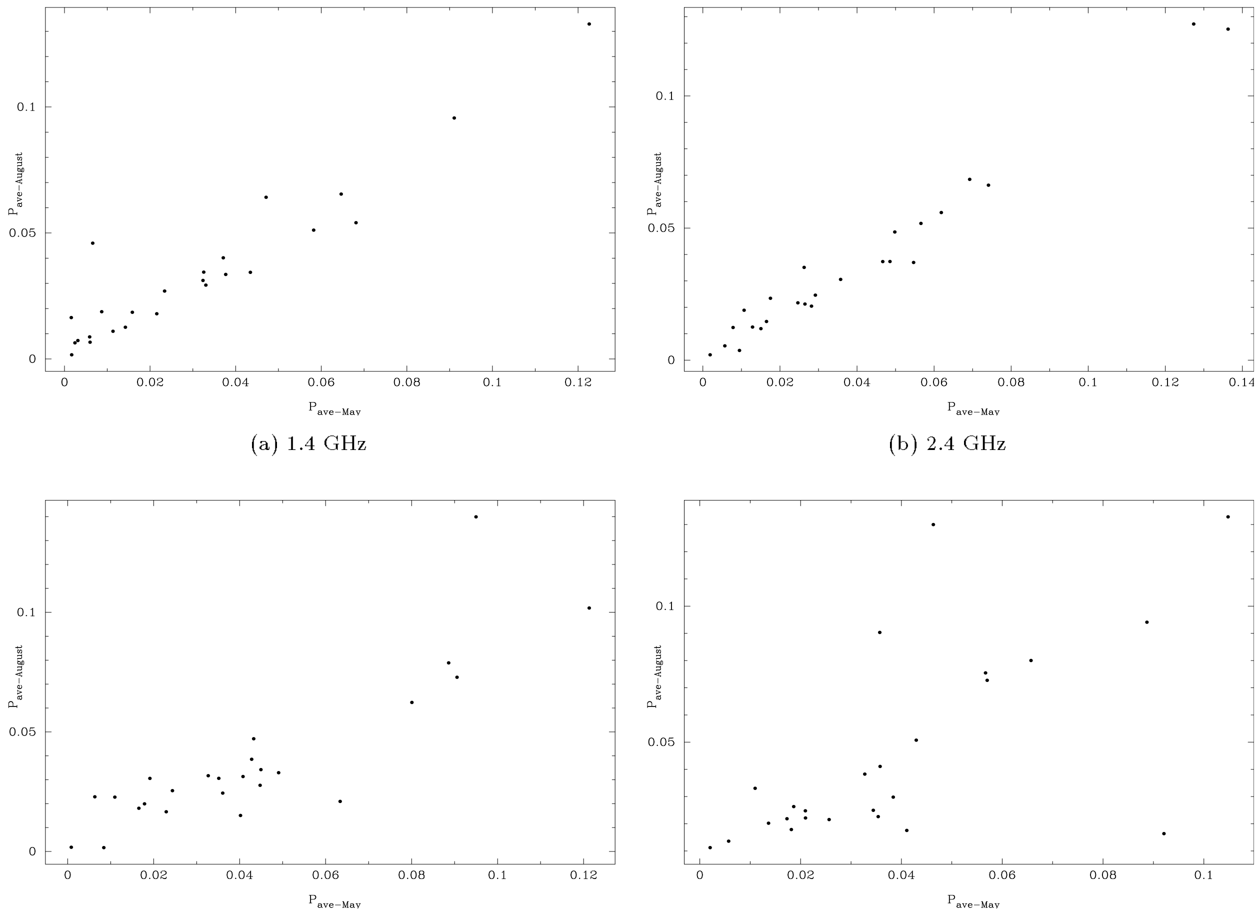

(a) 1.4 GHz

(b) 2.4 GHz

(c) 4.8 GHz

(d) 8.6 GHz

Figure 10: The scatter plot of average polarized flux density in May versus August 1994

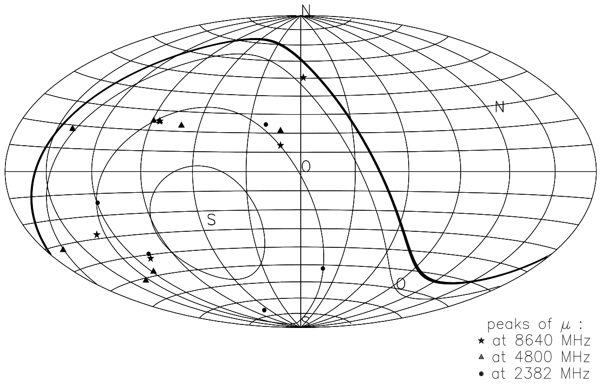

(a)

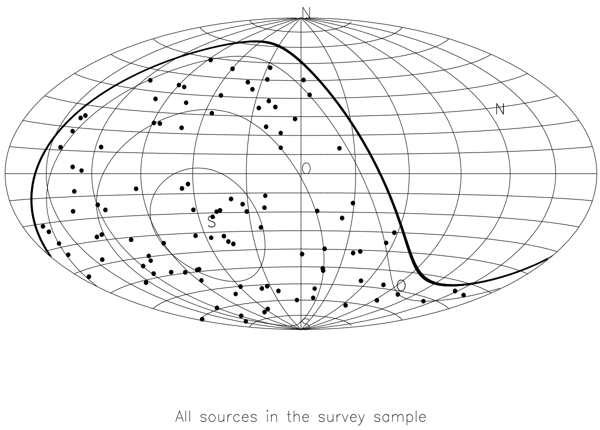

(b)

Figure 11: Distribution in respect to Galactic plane, of the IDV sources which show the peak of variability at given frequency (a) as compared with the distribution of the whole sample in Galactic coordinates (b). Data points are shown for May 1994. The total number of sources at different frequencies varies, only sources satisfying 'pointlikeness' criteria (see Table ??) were included. The 1.4 GHz data is not included here due to the larger uncertainties in flux density measurements. The thick curve shows the limits of the Survey, $\delta = +10°$.

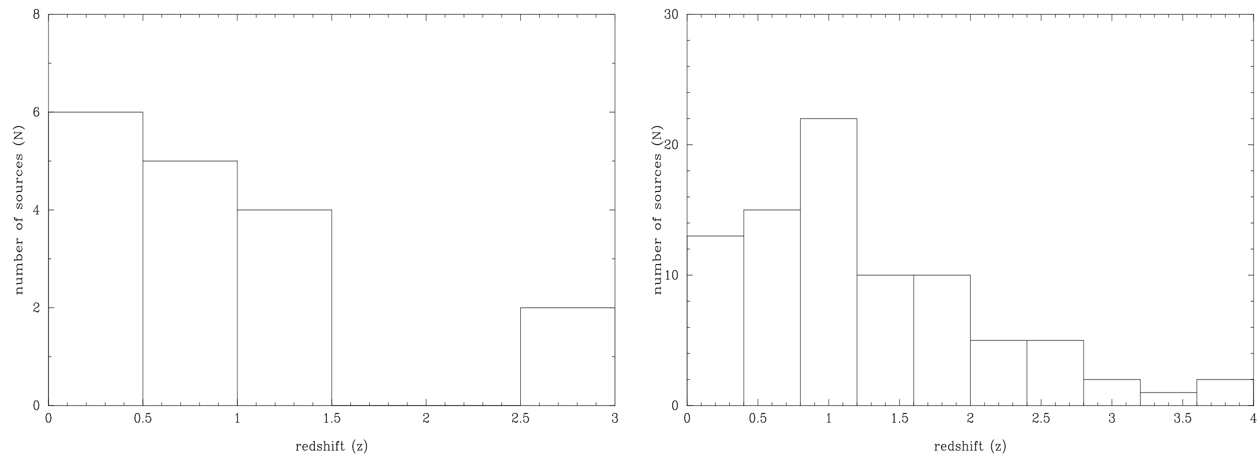

(a) IDV sources

(b) Whole sample

Figure 12: Redshift distribution of IDV sources compared with the whole sample. Sources with unknown redshift were excluded.